

A Treatment of the Coplanar Three-Beam Si[000, 440, 404] Diffraction*

BY O. PACHEROVÁ AND R. BUBÁKOVÁ

Institute of Physics, Czechoslovak Academy of Sciences, 180 40 Praha 8, Na Slovance 2, Czechoslovakia

(Received 12 February 1986; accepted 20 August 1986)

In memory of Professor Paul P. Ewald

Abstract

The peak of the spectral line Ni $K\alpha_2$ was measured by the double-crystal spectrometer in the arrangement (Si 440 sym., +Si 440 sym.). It is possible to adjust the Si crystal so that the conditions for coplanar three-beam Si[000, 440, 404] diffraction are satisfied for the wavelength of the incident radiation $\lambda \sim 0.166288$ nm involved in the Ni $K\alpha_2$ peak. When the second Si crystal was adjusted to this three-beam diffraction position an anomalous change of the measured dependence was found. A very simple model of the experiment was suggested and the necessary calculation completing the paper of Graeff & Bonse [*Z. Phys. B*, (1977), 27, 19-32] was performed to explain qualitatively the anomalous change.

1. Introduction

Nearly seventy years ago P. P. Ewald published the first of his admired papers on the dynamical theory of the diffraction of X-rays. Many investigators were able to use his theory to understand the details of X-ray diffraction in perfect or nearly perfect crystals, and even now investigators find in Ewald's work much inspiration for the solution of diffraction problems.

One of the problems arising from the dynamical theory which are studied in our laboratory is coplanar many-beam diffraction. An investigation of this forms the subject of the present paper. Ewald himself was very interested in many-beam diffraction problems (Ewald & Héno, 1968; Héno & Ewald, 1968). The most recent information about progress in this field can be found in *Multiple Diffraction of X-rays in Crystals* (Chang, 1984).

Coplanar three-beam Si[000, 440, 404] diffraction was first mentioned by Deslattes (1968) and was later examined by Graeff & Bonse (1977) from an interferometric point of view. The experimental part of our treatment of Si[000, 440, 404] was presented briefly at the Eleventh International Congress of Crystallography in Warsaw (Bubáková & Pacherová,

1978). In this paper we present the details of our experiment together with an explanation based on the dynamical theory.

2. Experiment

Coplanar three-beam Si[000, 440, 404] diffraction was investigated by a precise double-crystal spectrometer (DCS) in the antiparallel arrangement. Both crystals in the spectrometer were dislocation-free silicon single crystals aligned for 440 diffraction.

Fig. 1 shows the situation in the plane of incidence when the DCS is ideally prepared for the measurement of the spectral dependence [Si 440, +Si(3) 440]* of the Ni $K\alpha_2$ line. The plane of incidence (identical with the plane of the figure) is common to all participating diffractions. In the ideal case normals to the diffracting planes $(110)_{C_1}$, $(110)_{C_2}$ and $(101)_{C_2}$ lie in the plane of incidence.

The measurement consists in the rotation of C_2 (throughout, C_1 , C_2 will be used to mean the crystal C_1 or the crystal C_2), which is in the coplanar three-beam diffraction position, around the vertical axis a_2 . While adjusting the DCS the following situations arise:

(1) In the parallel arrangement (Si 440, -Si 440) information about the parallel positions of $(110)_{C_1}$ and $(110)_{C_2}$ is found.

* The symbol Si(3) means the Si crystal adjusted to the coplanar three-beam Si[000, 440, 404] diffraction position.

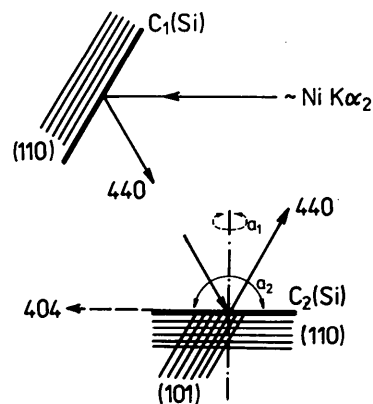


Fig. 1. Schematic drawing in the plane of incidence of the double-crystal spectrometer used in the experiment.

* This paper should be regarded as forming part of the Ewald Memorial Issue of *Acta Cryst.* Section A published in November 1986. The manuscript was received in its final form too late for inclusion.

(2) C_2 is driven back to the (440, +440) position.

(3) The DCS is at this moment set so that the radiation falls on the flank of C_2 . Then it is very slowly rotated with C_2 around the axis a_1 . The moment when C_2 goes through the position in which the (101) $_{C_2}$ planes are parallel to the (110) $_{C_1}$ planes is manifested by an increase in intensity of the (440, -404) reflection.

(4) The device is not equipped for automatic rotation around the a_1 axis. The manual adjustment of C_2 to the correct position is the most delicate operation of the whole experiment. The adjustment is evaluated by the shape of the (440, -404) rocking curve in comparison with the ideally adjusted (440, -440) rocking curve (point 1).

(5) When C_2 is considered to have been adjusted to the coplanar three-beam Si[000, 440, 404] position, the DCS is slightly turned so that the radiation falls only on the (110) surface sufficiently far from every other surface to satisfy the semi-infinite crystal condition.

(6) C_2 is rotated automatically by steps or manually (according to the size of the angle at which the measurement is performed) and so the spectral dependence [440, +(3)440] is obtained.

(7) With the automatic measurement C_2 returns from the end point to the starting point and the measurement is repeated at least twice.

(8) The device is returned to point 1 and a subsequent attempt to improve the adjustment of C_2 to the coplanar three-beam Si[000, 440, 404] diffraction takes place.

(9) The equivalent positions of Si(3) - Si[000, 440, 044], Si[000, 440, 404] and Si[000, 440, 044] - may be obtained by appropriate rotation of C_2 around the axis a_1 . The measurement of the spectral dependence [Si 440, +Si(3) 440] was repeated for these equivalent positions.

(10) Several times during the experiment the counter was set for the detection of the extremely asymmetrical reflection 404 (or 044, 404 and 044). No reflected energy was registered in these cases.

The device guarantees that for all operations described above (1-8) the normals to the (110) $_{C_1}$ and (110) $_{C_2}$ planes lie in the plane of incidence within limits of $\pm 1.5''$. The angle between the two positions of C_2 [(440, +440) and (440, -440)] is measured with an accuracy better than $1''$. The automatic rotation of C_2 around the axis a_2 can be performed by steps of 0.1, 0.2, 0.4 or 0.8''. The pulse summation time of the scintillation counter is automatically controlled by the registration device.

In Fig. 2(a) the whole [Si 440 sym., +Si(3) 440 sym.]/Ni $K\alpha_2$ rocking curve is shown (the angle of rotation of C_2 was 1620'' for this measurement) and in Fig. 2(b) the part around the anomalous behaviour is shown (30'' of the rotation of C_2). The curve of Fig. 2(b) was measured automatically point by point in

steps of 0.2'' and every point was registered for 1 min. For the shift to the subsequent point we had a break of 6 s during which the registration was halted. The shifting itself lasted 1.5 s. The interval $\Delta\lambda = 5 \times 10^{-6}$ nm* corresponds to an angle of rotation of C_2 of 21.5'' [and similarly $\Delta\lambda = 10^{-4}$ nm (Fig. 2a) \Leftrightarrow 429.7'']. 150 steps were needed for the 30'' interval of Fig. 2(b). The drawn curve is placed between the experimental points so that the maximum of the relative departure of the experimental points from the curve is about $\pm 2\%$. The anomalous curve was obtained over a period of 2.75 h. The room temperature was constant to ± 0.1 K during the measurement.

3. Theory

The coplanar three-beam Si[000, 440, 404] diffraction was calculated on the basis of the fundamental equations of dynamical diffraction in the arrangement given by Penning & Polder (1968) (henceforth PP).

* The explanation of the conversion $\Delta\lambda/\Delta\theta$ is as follows. The rotation of C_2 of the dispersive DCS in the plane of incidence causes a shift of the spectral window. For a general arrangement ($n, \mp m$) of the DCS the following relation holds:

$$|\Delta\lambda| = \lambda \Delta\theta / |\tan \theta_n \mp \tan \theta_m|$$

($\Delta\theta$ = angle of the rotation of C_2 , θ_n, θ_m = Bragg angles of diffractions n, m for the wavelength λ). This relation can be very easily and intuitively derived by means of the corresponding DuMond diagram. In the [Si 440, +Si(3) 440] case studied it is $|\Delta\lambda| [10^{-6} \text{ nm}] = 0.232 \Delta\theta [\text{arc sec}]$.

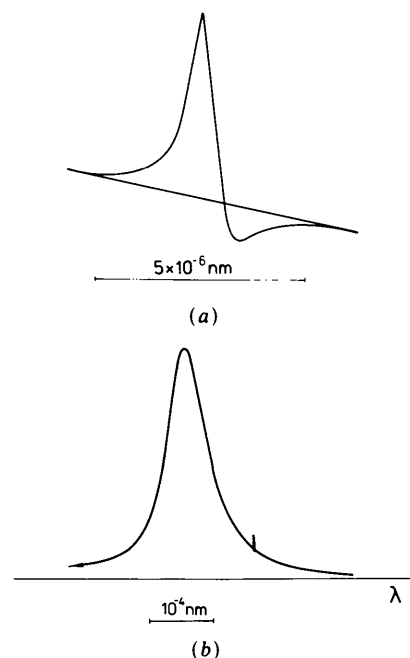


Fig. 2. (a) The [Si 440 sym., +Si(3) 440 sym.]/Ni $K\alpha_2$ rocking curve with the anomaly caused by the coplanar three-beam Si[000, 440, 404] adjustment of the second crystal. (b) The anomaly on the [440, +(3) 440] rocking curve. There are 150 experimental points lying on the anomaly.

The PP treatment is in accordance with our previous studies of coplanar many-beam diffractions (Pacherová, 1979; Pacherová & Bubáková, 1982; Pacherová & Bubáková, 1984), and seems to be entirely adequate in this case.

The fundamental equations of the dynamical solution of n -beam diffraction [PP, equation (3.8)] can be arranged for coplanar diffraction as follows:

$$\sum_{j=1}^n A_{ij} Y_j = 0, \quad (1)$$

$$\sum_{j=1}^n A_{ij}(\mathbf{u}_i \cdot \mathbf{u}_j) X_j = 0, \quad i = 1, 2, \dots, n. \quad (2)$$

X_j , Y_j are the amplitudes of the π , σ polarization components respectively of the dielectric displacement \mathbf{D}_j inside the diffracting crystal; $A_{ij(i \neq j)} = \psi_{ji}$; $A_{ii} = \psi_0 - 2(\mathbf{u}_i \cdot \Delta)/k_m$; ψ_{ij} is the term in the Fourier sum of the polarizability per unit volume corresponding to the reciprocal-lattice vector $\mathbf{b}_{ij} = \mathbf{k}_j - \mathbf{k}_i$; \mathbf{u}_i is the unit vector parallel to the vacuum wave vector \mathbf{k}_i , $\mathbf{k}_i = k_m \mathbf{u}_i$; Δ is the deviation of the centre of the reflection sphere from the Laue point.

We define the quantity $\Delta k = k - k_m$ which describes the change of the wavelength of the incident radiation. It was shown by Pacherová & Bubáková (1984, Appendix A4) that all equations resulting from (1) and (2) valid for $k = k_m$ hold also for $k \neq k_m$ if the quantity ψ_0 is substituted by $\psi_{0\text{ef}} = \psi_0 + 2\Delta k/k$.

4. Calculation

The Ewald geometrical construction of Si[000, 440, 404] is given in Fig. 3 in which \mathbf{u}_1 , \mathbf{u}_2 , \mathbf{u}_3 and Δ from (1) and (2) are introduced and the coordinate system xz in the plane of incidence together with the surface normal \mathbf{v} are shown.

In the case of Si[000, 440, 404] $\psi_{ij} = \psi_{440}$ and $\mathbf{u}_i \cdot \mathbf{u}_j = -0.5$ for all i, j ($i, j = 1, 2, 3, i \neq j$). Therefore we can solve both sets of equations (1) and (2) with the single set of equations

$$\sum_{j=1}^3 B_{ij} Z_j = 0, \quad i = 1, 2, 3 \quad (3)$$

in which

$$\begin{aligned} B_{ij(i \neq j)} &= B = \psi_{440} && \text{for } \sigma \text{ polarization} \\ B_{ij(i \neq j)} &= B = -0.5\psi_{440} && \text{for } \pi \text{ polarization} \\ B_{ii} &= A_{ii} \\ Z_i &= Y_i && \text{for } \sigma \text{ polarization} \\ Z_i &= X_i && \text{for } \pi \text{ polarization.} \end{aligned}$$

To unify the notation we will write $B_0 = \psi_{0\text{ef}}$.

The secular equation of Si[000, 440, 404] is

$$B_{11} B_{22} B_{33} - B^2 (B_{11} + B_{22} + B_{33}) + 2B^3 = 0. \quad (4)$$

By expressing B_{ii} in x, z coordinates (4) leads to

$$\begin{aligned} 3(2x - kB_0)z^2 - 2x^3 - 3B_0 kx^2 \\ + k^3(2B^3 - 3B^2 B_0 + B_0^3) = 0, \end{aligned}$$

i.e.

$$z_{1,2} = \pm \{ [2x^3 + 3B_0 kx^2 - k^3(2B^3 - 3B^2 B_0 + B_0^3)] / [3(2x - kB_0)] \}^{1/2}. \quad (5)$$

Three asymptotes of the dispersion curves (5) are:

$$x = 0.5kB_0, \quad (6)$$

$$z = \pm 3^{1/2}(x + kB_0)/3. \quad (7), (8)$$

When we use the above procedure on the two-beam Si[000, 440] and Si[000, 404] diffractions we obtain the following:

(a) Si[000, 440]: The secular equation $B_{11} B_{22} = B^2$ is expressed in x, z coordinates as

$$z_{1,2} = \pm \{ [(x + kB_0)^2 - k^2 B^2] / 3 \}^{1/2} \quad (9)$$

with asymptotes

$$z = \pm 3^{1/2}(x + kB_0)/3 \quad [\text{cf. (7), (8)}].$$

(b) Si[000, 404]: In this case the dispersion equation is

$$\begin{aligned} z = 3^{1/2} [2x^2 + kB_0 x \\ + k^2(B^2 - B_0^2)] / [3(2x - kB_0)] \quad (10) \end{aligned}$$

and its asymptotes are

$$x = 0.5kB_0 \quad \text{and} \quad z = 3^{1/2}(x + kB_0)/3 \quad [\text{cf. (6), (7)}].$$

We can see that the three asymptotes of the three-beam dispersion curve are the same as the three asymptotes of the two corresponding two-beam dispersion curves.

Some interesting properties of the dispersion curves arise from the following arrangement of equations (5) and (9). We can rewrite these in the forms

$$z_{1,2} = \pm \{ (x - x_1)(x - x_2)(x - x_3) / [3(x - x_4)] \}^{1/2} \quad (5a)$$

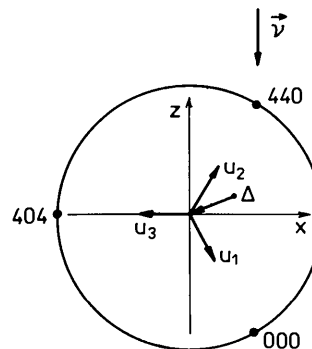


Fig. 3. Ewald's geometrical construction for the coplanar three-beam Si[000, 440, 404] diffraction. The definition of the basic vectors and the system of coordinates used in the calculation is shown.

where

$$\left. \begin{aligned} x_1 &= -k(B_0 - B) \\ x_2 &= -k\{B_0 + 2B + [(3B_0 + 2B)^2 - 16B^2]^{1/2}\}/4 \\ x_3 &= -k\{B_0 + 2B - [(3B_0 + 2B)^2 - 16B^2]^{1/2}\}/4 \\ x_4 &= 0.5kB_0 \end{aligned} \right\} \quad (5b)$$

$$z_{1,2} = \pm[(x - \xi_1)(x - \xi_2)/3]^{1/2} \quad (9a)$$

where

$$\left. \begin{aligned} \xi_1 &= -k(B_0 - B) \\ \xi_2 &= -k(B_0 + B) \end{aligned} \right\} \quad (9b)$$

The values of $x = x_{1,2,3}$ or $x = \xi_{1,2}$ satisfy the condition $z_{1,2} = 0$. In the case of the two-beam Si[000, 440] diffraction the values of $x = \xi_{1,2}$ coincide with the

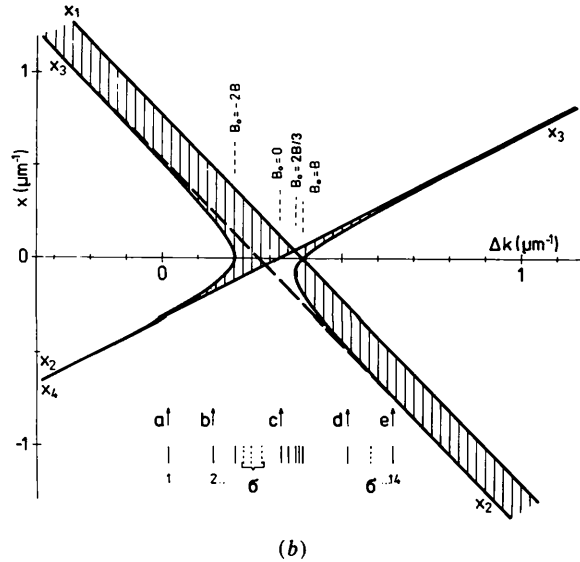
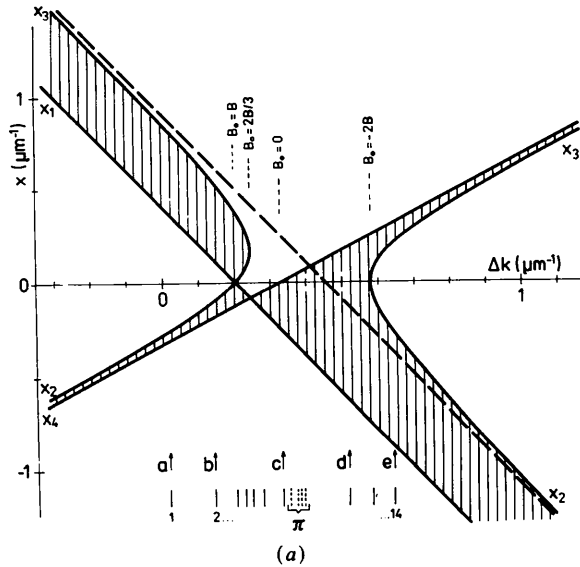


Fig. 4. The Δk dependence of $x_{1,2,3,4}$ and $\xi_{1,2}$ illustrating the character of the Si[000, 440, 404] dispersion surface. See text. (a) σ polarization, (b) π polarization.

vertices of the dispersion hyperbola. Two of the three intersections of the three-beam dispersion curve (5a) with the axis x can be joined to the vertices $\xi_{1,2}$. They are $x_1 \equiv \xi_1$ and $x_{3 \text{ or } 2} \sim \xi_2$ (see Fig. 4). We notice that $\xi_1 < \xi_2$ for σ polarization but $\xi_2 < \xi_1$ for π polarization.

The values of $x_{1,2,3,4}$ restrict the ranges of total reflections of Si[000, 440, 404]. Owing to the Δk dependence of B_0 they are functions of Δk as well. It is simple to pass from $x_{1,2,3,4}(\Delta k)$ to the functions $x'_{1,2,3,4}(\Delta \lambda)$ which appear in the DuMond diagram. For this purpose we need:

$$\begin{aligned} \lambda_m &= 2\pi/k_m, \quad \Delta \lambda/\lambda_m = -\Delta k/k_m, \\ \Delta \theta &= 2\sqrt{3} \Delta x/(3k_m) \end{aligned} \quad (11)$$

(the angular measure showing the shift Δx of the tie points along the dispersion surface if the angle of incidence of the incident wave changes about $\Delta \theta$) and

$$x'_i = -(x_i + 0.5\Delta k) \quad (12)$$

(the minus sign follows from the fact that C_2 is in the antiparallel position relative to C_1).

In the simplest model of our experiment the anomalous behaviour is explained by the Δk dependence of the size of the spectral window ($C_1 \times C_2$), i.e. the reflection coefficient is considered to equal 1 if the angle of incidence belongs to the range of total reflection, elsewhere it is equal to 0. The vertical divergence of the incident beam is considered to be zero.

5. Results

The constants used in our calculation were as follows:

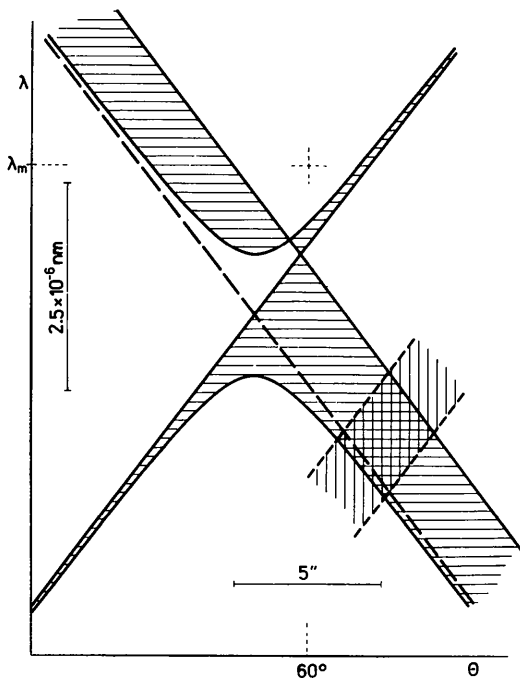
$$\begin{aligned} a_0 &= 0.543095 \text{ nm} \quad (\text{lattice constant}) \\ F_0 &= 112 \quad (F_{HKL} \text{ terms of the Fourier} \\ F_{440} &= 42.80 \quad (\text{sum of the structure factor}). \end{aligned}$$

The derived quantities used in the calculation are

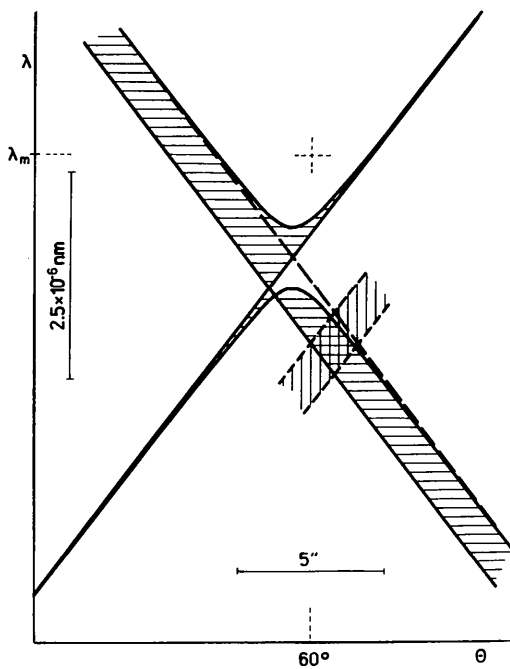
$$\begin{aligned} k_m &= 37.7849 \text{ nm}^{-1}, \\ \lambda_m &= 0.166288 \text{ nm}, \quad \psi_0 = -1.734 \times 10^{-5}, \\ \psi_{440} &= -0.663 \times 10^{-5}. \end{aligned}$$

Fig. 4 shows the Δk dependence of the values of $x_{1,2,3,4}$ [equation (5b)] and of $\xi_{1,2}$ [equation (9b)], $\xi_1 \equiv x_1$, $\xi_2 =$ dashed line]. The ranges of total reflections are indicated by the hatching. Several values of Δk for which the character of the dispersion curve intersect at one point. Arrows $a-e$ show the values of Δk which correspond to the pictures of the cuts through the plane of incidence of the dispersion

surface defined by Graeff & Bonse (1977). The lines below mark values of Δk for which the same pictures are drawn together with the angular dependences of the reflection coefficient in Fig. 8.



(a)



(b)

Fig. 5. The spectral window of the [440, +(3) 440] arrangement of the double-crystal spectrometer. (a) σ polarization, (b) π polarization.

The spectral window for one arrangement of C_1 and C_2 of the [Si 440 sym., +Si(3) 440 sym.] experiment is shown in Fig. 5 [equations (12), (11) and $\xi'_{1,2} = \xi_{1,2} + 0.5 \Delta k$ were used in drawing Fig. 5].

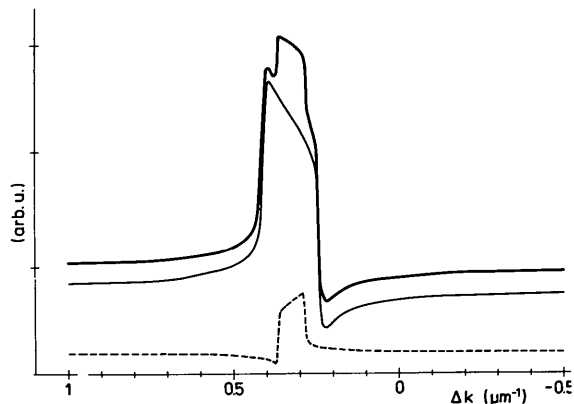


Fig. 6. The Δk dependence of the size of the spectral window. Dashed line: π polarization; full line: σ polarization; thick line: the resultant ($\sigma + \pi$) dependence.

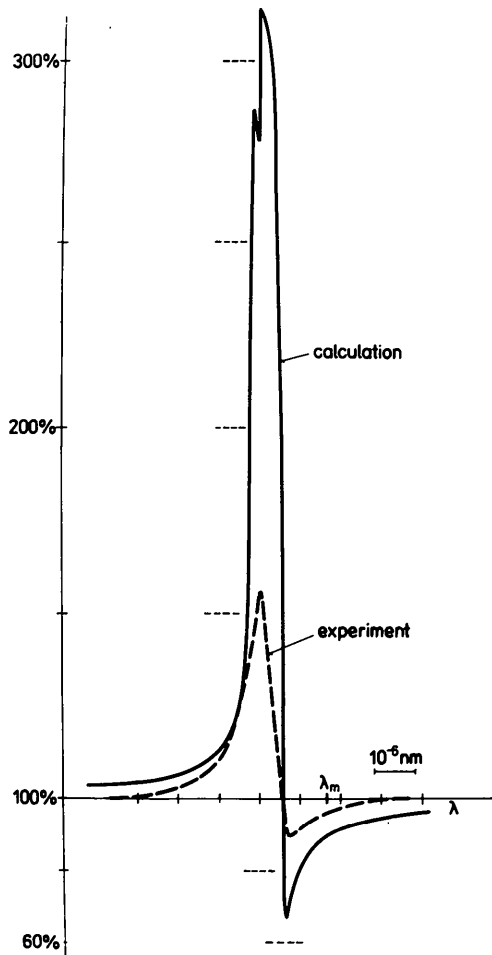


Fig. 7. Comparison of the calculated and the experimental anomaly arising on the [Si 440 sym., +Si(3) 440 sym.]/Ni $K\alpha_2$ rocking curve when the second crystal is adjusted to the coplanar three-beam Si[000, 440, 404] diffraction position.

The Δk dependence of the size of the spectral window (Fig. 5) is shown in Fig. 6. Fig. 7 compares the calculated and the experimental anomalous behaviour of the studied rocking curve. The value of 100% corresponds to the case when C_2 is in the obvious two-beam Si[000, 440] diffraction position.*

6. Concluding remarks

The calculated [Si 440 sym., +Si(3) 440 sym.]/Ni $K\alpha_2$ rocking curve qualitatively agrees with the experimental one. It is very likely that the quantitative discrepancy is due to a non-ideal adjustment of C_2 to the coplanar Si[000, 440, 404] position (the anomalous behaviour of the rocking curve was very

* The experimental curve was put on the λ axis so that the maximum values of the experimental and the calculated curves could be achieved at the same value of λ . The experimental determination of the position of λ_m is limited by the accuracy of the determination of the position of λ (Ni $K\alpha_2$). We estimate this accuracy is about $\Delta\lambda = \pm 0.6 \times 10^{-6}$ nm in our experiment, which corresponds to the size of the angle of rotation of C_2 of $\Delta\theta = \pm 2.5''$.

sensitive to the adjustment within limits of $1'$). Another reason for the quantitative discrepancy is undoubtedly our simple model of the experiment which ignores the vertical divergence.

APPENDIX A

Dispersion surface

Several examples of cuts through the plane of incidence of the dispersion surface are given in Fig. 8. The scale on the x axis is shown in Fig. 8(a); the scale on the z axis (not shown) is the same as that on the x axis. The centre of the range of total reflection of the two-beam Si[000, 440] diffraction is marked by x_c . The thick lines indicate the branches of the dispersion surface excited when the surface normal is oriented from the top down.

Note the interesting property of the dispersion surface in Figs. 8(b)-(e) for σ polarization and in Figs. 8(i)-(l) for π polarization: the central part of the dispersion surface first decreases to a point and

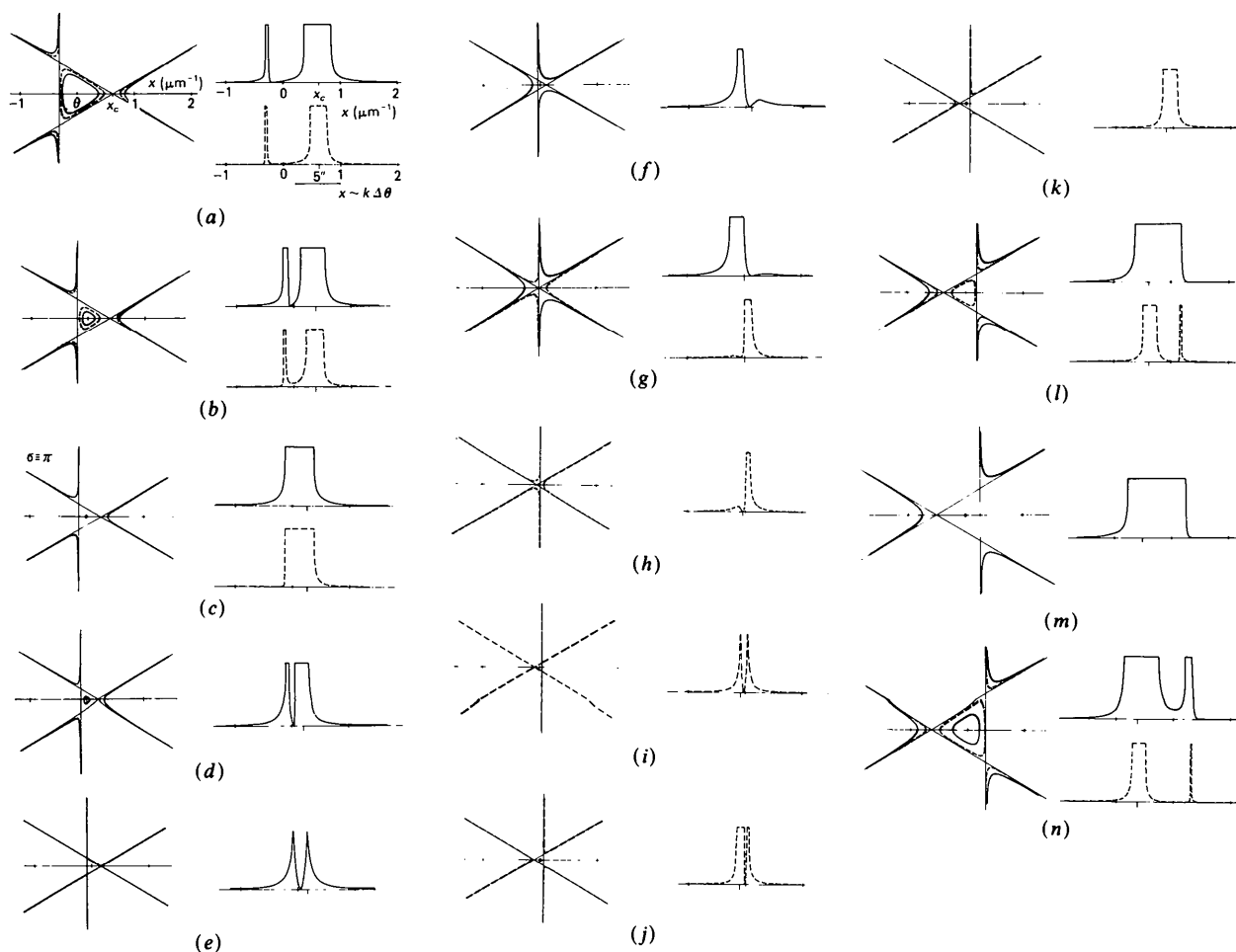


Fig. 8. The dispersion surface in the plane of incidence of the coplanar three-beam Si[000, 440, 404] diffraction for several values of Δk (for their estimates see Fig. 4). The dependences of the reflection coefficient correspond to the illustrated dispersion surfaces. The interval of Δk to which Fig. 8 belongs is $\Delta k \in (0, 0.65) \mu\text{m}^{-1}$. Dashed lines: π polarization; full lines: σ polarization.

after that it again enlarges but with the opposite orientation of the Poynting vector. A further interesting property can be found in Figs. 8(e) (σ) and in 8(i) (π). The values of Δk for the cases drawn imply $x_1 = x_4$ and $x_2 = x_3$. The dispersion surface in the plane of incidence is created by the three lines identical with the asymptotes. The last interesting property we wish to point out is illustrated in Fig. 8(c). The dispersion surface in the plane of incidence is identical for σ and π polarizations.

APPENDIX B

Reflection coefficient

We define the reflection coefficient according to James (1963) as

$$R = |Z_2|^2 / |Z_1|^2 \quad (13)$$

for the symmetrical reflection 440; for the extremely asymmetrical reflection 404 the formula used leads to zero. It was found (e.g. Bedyńska, 1973; Colella, 1982) that in cases of extremely asymmetrical reflections linearization of the coefficients of the dynamical equations is not permissible. We added to the coefficients A_{ij} from (1) and (2) the term $-(\Delta \cdot \Delta) / k_m^2$ and calculated for $k = k_m$ the dispersion surface in this more accurate approach. The result of this calculation gives us in the $3 \mu\text{m}^{-1}$ neighbourhood of the Laue point a picture of the dispersion surface nearly identical with that calculated according to (5) (the shift in the values of $x_{1,2,3}$ is of the order of $10^{-5} \mu\text{m}^{-1}$). We conclude that the dependences illustrated in Fig. 5 would stay unchanged in the more accurate approach. For this reason we can also expect that the resultant dependences shown in Figs. 6 and 7 are valid.

Acta Cryst. (1987). **A43**, 167–173

Random Elastic Deformation (RED) – an Alternative Model for Extinction Treatment in Real Crystals*

BY J. KULDA

Nuclear Physics Institute, Czechoslovak Academy of Sciences, 250 68 Řež near Prague, Czechoslovakia

(Received 30 December 1985; accepted 3 September 1986)

Abstract

A modification of the Hamilton–Zachariasen theory of extinction in imperfect crystals is reported. Unlike

* This paper should be regarded as forming part of the Ewald Memorial Issue of *Acta Cryst.* Section A published in November 1986. The manuscript was received in its final form too late for inclusion.

No great problems arose when we attempted to proceed in the obvious way to apply the boundary conditions and also to calculate the reflection coefficient with the linearized coefficients A_{ij} . The formula derived from (13) for Si[000, 440, 404] and the 440 reflection

$$R_{440} = B^2(B_{33} - B)^2 / (B_{22}B_{33} - B^2)^2 \quad (14)$$

does not lead to physically impossible or to apparently improbable results.

Several examples of the reflection coefficient R_{440} are shown together with the corresponding dispersion surfaces in Fig. 8. The angular scale given in Fig. 8(a) follows from (11). The reflection coefficient R_{440} equals one for the ranges of total reflection. The only point for which the calculation using the linearization is indefinite is $x = x_4$ and Δk such that $B_0 = 2B/3$ [Fig. 8(e) (σ) and Fig. 8(i) (π)]. From the continuity of R_{440} we established $R_{440} = 1$ at this point.

References

- BEDYŇSKA, T. (1973). *Phys. Status Solidi A*, **19**, 365–372.
 BUBÁKOVÁ, R. & PACHEROVÁ, O. (1978). *Acta Cryst.* **A34**, S233.
 CHANG, S. L. (1984). *Springer Series in Solid-State Sciences*, Vol. 50. Berlin: Springer.
 COLELLA, R. (1982). *Z. Naturforsch. Teil A*, **37**, 437–447.
 DESLATTES, R. D. (1968). *Appl. Phys. Lett.* **12**, 133–135.
 EWALD, P. P. & HÉNO, Y. (1968). *Acta Cryst.* **A24**, 5–15.
 GRAEFF, W. & BONSE, U. (1977). *Z. Phys. B*, **27**, 19–32.
 HÉNO, Y. & EWALD, P. P. (1968). *Acta Cryst.* **A24**, 16–42.
 JAMES, R. W. (1963). *Solid State Phys.* **15**, 53–220.
 PACHEROVÁ, O. (1979). Thesis. Czechoslovak Academy of Sciences.
 PACHEROVÁ, O. & BUBÁKOVÁ, R. (1982). *Z. Naturforsch. Teil A*, **37**, 617–625.
 PACHEROVÁ, O. & BUBÁKOVÁ, R. (1984). *J. Appl. Cryst.* **17**, 375–384.
 PENNING, P. & POLDER, D. (1968). *Philips Res. Rep.* **23**, 1–12.

the generally adopted Darwin mosaic model the crystal is supposed to consist of elastically deformed domains so that individual reflection events can be treated within the quasiclassical approach developed by the author in an earlier study [*Acta Cryst.* (1984), **A40**, 120–126]. In this way a modified expression for the scattering cross section, taking into account multiple wave interference, is introduced into the